Research Journal of Applied Sciences, Engineering and Technology 6(4): 748-753, 2013
DOI:10.19026/rjaset.6.4191
ISSN: 2040-7459; e-ISSN: 2040-7467

Submitted: December 3, 2012 Accepted: January 01, 2013 Published: June 20, 2013

Research Article

Asymmetrical Fault Ride through based on Predictive Current Control in Wind Power Generation System

[1]Li Yuren, [1, 2]Zhang Junli, [1]Zhang Zhihui and [1]Fu Longfei
[1]Northwestern Polytechnical University, Xi'an 710007, China
[2]Baoji University of Arts and Sciences 721013, China

Abstract: In order to improve the asymmetric fault ride-through capability of wind power generation system, asymmetric voltage and current can be decomposed into positive sequence, negative sequence and zero sequence components respectively via symmetrical component method. The mathematical models of grid side converter in static coordinate system and synchronous rotating coordinate system were given; predictive current control strategy proposed can achieve no static error tracking of current in each switching cycle, can eliminate the negative sequence current in asymmetric fault and wipe off the secondary ripple of the dc side capacitor voltage. The dc side super-capacitor circuit can prevent the dc side from over-voltage. The methods introduced in this study can improve the large grid asymmetric fault ride through capability of wind power generation system. Effectiveness of the proposed methods is verified by the numerical simulations.

Keywords: Asymmetric fault, grid side converter, predictive current control, symmetrical components, wind power generation system

INTRODUCTION

Wind power generation is considered to be one of the fastest growing renewable energy sources. Differently from double feed induction generator wind power system, permanent magnet direct drive wind power system has many advantages such as no gearbox, high power density, high precision, simple control strategy, not requiring pre-installation cost (Chinchilla *et al*., 2006; Polinder *et al*., 2006). With the increasing scale of wind farms, the connection state of wind power generation system and grid has become more and more important. In recent years, some countries have already issued the grid codes of wind power generation system connecting with the grid (Iov *et al.*, 2007; Saniter and Janning, 2008). The effective power management in micro grid and smart grid had been reported (Jeon *et al*., 2006; Lima *et al*., 2010), in which the grid voltage fluctuations are more epidemic than traditional systems. Therefore, the grid fault ride through capacity of wind power generation system must be considered.

Grid codes require that wind power generation system to have certain low voltage ride through capability. With the grid codes in many countries, wind power generation system should stay connected to the grid during its voltage fault to help the grid to restore regular voltage. In the electrical power system with higher proportion of wind power generation system, the power supply outage will occur if the wind power generation system trip off the grid. The low voltage ride through requirements that wind power generation system should keep connected to the grid during its voltage sags are shown in Fig. 1 (Iov *et al*., 2007). The asymmetric grid fault will bring many problems: the negative sequence current in grid side converter ac side resulting in the three phase current asymmetry; 2 times fundamental frequency fluctuations in grid side converter dc. The dc side voltage fluctuations will cause the 3rd harmonic in ac input current which will pollute the power grid and damage other electricity equipments. The dc voltage fluctuations will cause frequently capacitor charging and discharging and reduce its life. Large fluctuations of dc side voltage in the grid side converter will cause system instability (Li and Xu, 2009). The traditional methods used mainly restrained negative sequence current and counterpoised three phase current, but they do not eliminate the dc side voltage ripple.

In this study the mathematical models of grid side converter in static coordinate system and synchronous rotating coordinate system were given and predictive current control strategy was introduced with its basis. Negative sequence current was regarded as the disturbance of positive sequence current in asymmetry three phase current and this strategy can effectively reduce the 2^{nd} ripple dc side voltage. The protection circuit in wind power generation system was introduced to prevent the dc side from over-voltage.

Corresponding Author: Li Yuren, Northwestern Polytechnical University, Xi'an 710007, China

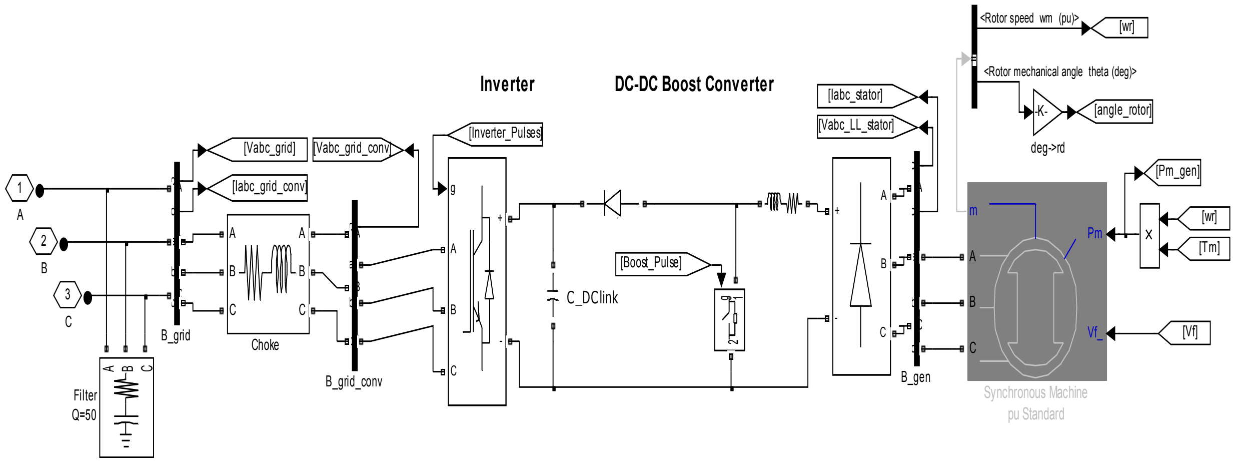

Fig. 1: The structure of wind power generation system

THE MATHEMATICAL MODEL OF GRID SIDE CONVERTER

Symmetrical component method is the linear transformation which can convert the asymmetry three phase voltages and currents into symmetrical three phase voltages and currents, Via symmetrical component method asymmetric three phase voltage can be disintegrated into symmetric positive sequence, negative sequence and zero sequence components and three parts are symmetric and independent of each other, facilitating the analysis of wind power generation system.

The mathematical model in stationary coordinate system: Via symmetrical component method, asymmetric three phase voltage can be disintegrated into symmetric positive sequence, negative sequence and zero sequence components. The mathematical model of grid side converter in the grid voltage asymmetry can be obtained according to its mathematical model in the grid voltage symmetry and symmetrical component method.

In two phase stationary coordinate system (Li and Xu, 2009), the voltage vector of grid is shown in (1):

$$\begin{aligned} E_{\alpha\beta} &= \frac{2}{3}[e_a + ae_b + a^2e_c] = e_\alpha + je_\beta \\ &= E^p{}_{\alpha\beta} + E^n{}_{\alpha\beta} = e^{j\omega t}E^p{}_{dq} + e^{-j\omega t}E^n{}_{dq} \\ &= e^p{}_\alpha + e^n{}_\alpha + j(e^p{}_\beta + e^n{}_\beta) \end{aligned} \tag{1}$$

The voltage vector of grid side converter is shown in (2):

$$\begin{aligned} U_{\alpha\beta} &= u_\alpha + ju_\beta \\ &= U^p{}_{\alpha\beta} + U^n{}_{\alpha\beta} = e^{j\omega t}U^p{}_{dq} + e^{-j\omega t}U^n{}_{dq} \\ &= u^p{}_\alpha + u^n{}_\alpha + j(u^p{}_\beta + u^n{}_\beta) \end{aligned} \tag{2}$$

The current vector of grid side converter is shown in (3):

$$\begin{aligned} I_{\alpha\beta} &= i_\alpha + ji_\beta \\ &= I^p{}_{\alpha\beta} + I^n{}_{\alpha\beta} = e^{j\omega t}I^p{}_{dq} + e^{-j\omega t}I^n{}_{dq} \end{aligned} \tag{3}$$

The ac circuit equation in two phase stationary coordinate system based on the topology of the grid side converter is shown in (4):

$$L\frac{dI_{\alpha\beta}}{dt} = E_{\alpha\beta} - U_{\alpha\beta} - RI_{\alpha\beta} \tag{4}$$

It can be seen in (4), $I_{\alpha\beta}$ can be controlled by controlling the ac voltage vector $U_{\alpha\beta}$ of grid side converter and this means that three phase current can be controlled.

The mathematical model in synchronous coordinate system: The state equation is shown in (5) according to the topology of grid side converter and its equation (Li and Xu, 2009):

$$\begin{cases} L\dfrac{di^p{}_d}{dt} = e^p{}_d - u^p{}_d - Ri^p{}_d + \omega Li^p{}_q \\ L\dfrac{di^p{}_q}{dt} = e^p{}_q - u^p{}_q - Ri^p{}_q - \omega Li^p{}_d \\ L\dfrac{di^n{}_d}{dt} = e^n{}_d - u^n{}_d - Ri^n{}_d - \omega Li^n{}_q \\ L\dfrac{di^n{}_q}{dt} = e^n{}_q - u^n{}_q - Ri^n{}_q + \omega Li^n{}_d \end{cases} \tag{5}$$

The state Eq. (5) of wind power generation system is based on the synchronous rotating coordinate system and the dual current closed loop control strategy can be designed according to (5). When the three-phase voltage is asymmetric, three phase complex power vector can be described as (6):

$$S = E_{\alpha\beta}\bar{I}_{\alpha\beta} = p(t) + jq(t) = (e^{j\omega t}E_{dq}^{d} + e^{-j\omega t}E_{dq}^{n})\overline{(e^{j\omega t}I_{dq}^{d} + e^{-j\omega t}I_{dq}^{n})} \tag{6}$$

The active power and reactive power is shown in (7):

$$\begin{cases} p(t) = p_0 + p_{c2}\cos(2\omega t) + p_{s2}\sin(2\omega t) \\ q(t) = q_0 + q_{c2}\cos(2\omega t) + q_{s2}\sin(2\omega t) \end{cases} \tag{7}$$

where, p_0 and q_0 is the average of active and reactive power, respectively, p_{c2} and p_{s2} is the secondary active power cosine, active power sine harmonic peak, respectively, q_{c2} and q_{s2} = Secondary reactive power cosine, reactive power sine harmonic peak, respectively. Eq. (7) is unfolded as (8):

$$\begin{cases} p_0 = \frac{3}{2}(e_d^p i_d^p + e_q^p i_q^p + e_d^n i_d^n + e_q^n i_q^n) \\ p_{c2} = \frac{3}{2}(e_d^p i_d^n + e_q^p i_q^n + e_d^n i_d^p + e_q^n i_q^p) \\ p_{s2} = \frac{3}{2}(e_q^n i_d^p - e_d^n i_q^p - e_q^p i_d^n + e_d^p i_q^n) \\ q_0 = \frac{3}{2}(e_q^p i_d^p - e_d^p i_q^n + e_q^n i_d^n - e_d^n i_q^n) \\ q_{c2} = \frac{3}{2}(e_q^p i_d^n - e_d^p i_q^n + e_q^n i_d^p - e_d^n i_q^p) \\ q_{s2} = \frac{3}{2}(e_d^p i_d^p + e_q^p i_q^p - e_d^n i_d^p - e_q^n i_q^p) \end{cases} \tag{8}$$

If p_0^*, p_{c2}^*, p_{s2}^*, q_0^* is the active power and reactive power command, respectively and $i_d^{p^*}, i_q^{p^*}, i_d^{n^*}, i_q^{n^*}$ is the corresponding current command respectively, the power commands can be obtained in (9):

$$\begin{bmatrix} p_0^* \\ q_0^* \\ p_{s2}^* \\ p_{c2}^* \end{bmatrix} = \frac{3}{2}\begin{bmatrix} e_d^p & e_q^p & e_d^n & e_q^n \\ e_q^p & -e_d^p & e_q^n & -e_d^n \\ e_q^n & -e_d^n & -e_q^p & e_d^p \\ e_d^n & e_q^n & e_d^p & e_q^p \end{bmatrix}\begin{bmatrix} i_d^{p^*} \\ i_q^{p^*} \\ i_d^{n^*} \\ i_q^{n^*} \end{bmatrix} \tag{9}$$

The current commands can be obtained in (10):

$$\begin{bmatrix} i_d^{p^*} \\ i_q^{p^*} \\ i_d^{n^*} \\ i_q^{n^*} \end{bmatrix} = \begin{bmatrix} e_d^p & e_q^p & e_d^n & e_q^n \\ e_q^p & -e_d^p & e_q^n & -e_d^n \\ e_q^n & -e_d^n & -e_q^p & e_d^p \\ e_d^n & e_q^n & e_d^p & e_q^p \end{bmatrix}^{-1}\begin{bmatrix} \frac{2}{3}p_0^* \\ \frac{2}{3}q_0^* \\ \frac{2}{3}p_{s2}^* \\ \frac{2}{3}p_{c2}^* \end{bmatrix} \tag{10}$$

PREDICTIVE CURRENT CONTROL STRATEGY

The predictive current control is method, which forces i_a, i_b, i_c in grid side converter follow the pre-given current command i_{ref} within one switching cycle. Transient voltage equation for the grid side converter topology of a phase is shown in (11) (Li and Xu, 2009):

$$e_a = L\frac{di_a}{dt} + Ri_a + u_a \tag{11}$$

The duty cycle in one switching cycle is d_a, d_b, d_c. The ac voltage and the dc capacitor voltage can be described as (12):

$$u_a = u_{dc}(d_a - \frac{1}{2}) \tag{12}$$

$$\frac{di_a}{dt} = \frac{i_{ref} - i_a}{T_s} \tag{13}$$

where, u_a is a phase voltage in grid side converter.

Supposed in one switching cycle, i_a follows i_{ref}, the rate of change in current is shown in (13). Where, T_s is the sampling period.

According to (11) to (13), the predicted current control law is obtained in (14):

$$d_a = \frac{1}{u_{dc}}\left[u_a - (R_s - \frac{L_s}{T_s})i_a - \frac{L_s}{T_s}\right] + \frac{1}{2} \tag{14}$$

Control switches according to the duty cycle in (14), the converter current will follow the current command correctly in one switching cycle. The positive and negative sequence command current, $i_d^{p^*}, i_q^{p^*}, i_d^{n^*}$, $i_q^{n^*}$ can be transformed into $i_{\alpha\beta}^*$ of two-phase stationary coordinate system and is shown in (15):

$$i_{\alpha\beta}^* = i_{\alpha\beta}^{p*} + i_{\alpha\beta}^{n*} = i_{dq}^{p*}e^{j\omega t} + i_{dq}^{n*}e^{-j\omega t} = i_\alpha^* + ji_\beta^* \tag{15}$$

This is the current value in next operation point predicted. The transform matrix C_{32} is equal amounts transformation. i_α and I_β in the $\alpha\beta$ coordinate system can be obtained according to 3/2 transforming of three-phase ac current.

$$C_{32} = \frac{2}{3}\begin{bmatrix} 1 & -\frac{1}{2} & -\frac{1}{2} \\ 0 & \frac{\sqrt{3}}{2} & -\frac{\sqrt{3}}{2} \end{bmatrix} \tag{16}$$

In the two-phase stationary coordinates system, the difference of given the current i_α^* and the actual current i_α can be obtained in a sampling period and ac inductance voltage can be obtained in (17):

$$u_{\alpha L} = L\frac{di_a}{dt} + Ri_a = L\frac{d(i_a^* - i_a)}{dt} + Ri_a \tag{17}$$

The α axis input voltage in grid side converter is shown in (18):

$$u_\alpha = e_\alpha - u_{\alpha L} \tag{18}$$

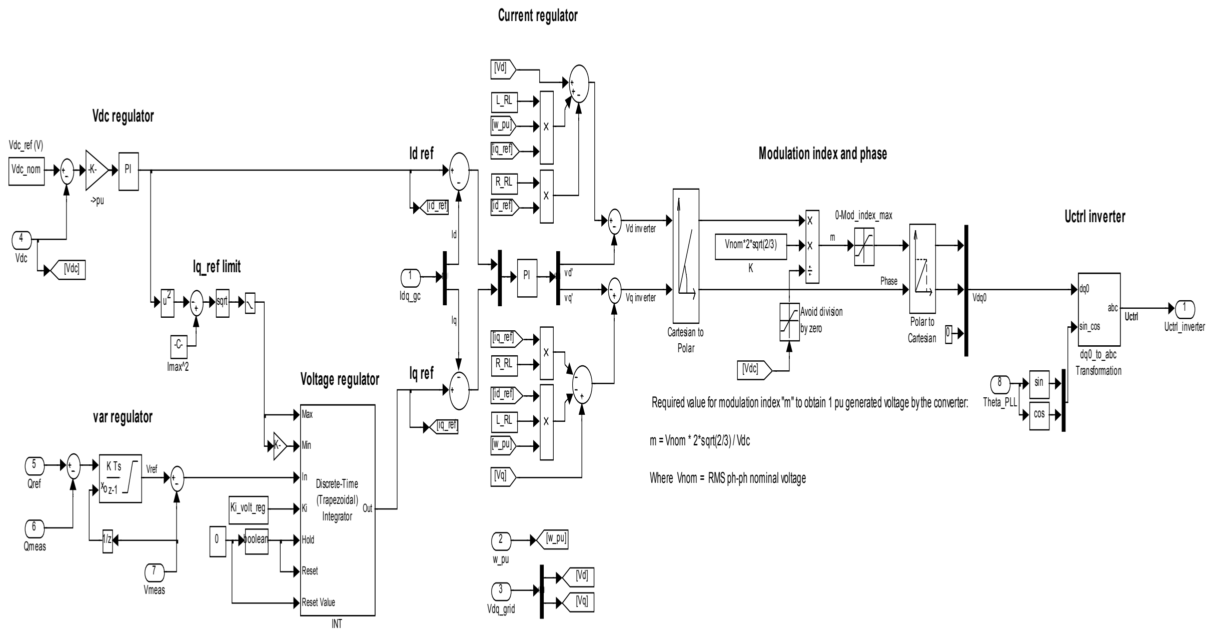

Fig. 2: The controller of grid side converter

Similarly, the β axis input voltage in grid side converter is in (19):

$$u_\beta = e_\beta - u_{\beta L} \tag{19}$$

The ac voltages in (18) and (19) in two-phase stationary coordinates is sent to SVPWM modulator. The output PWM pulses regulate grid side converter to achieve ultimate control purposes, the control block diagram in Fig. 2 (Li and Xu, 2009).

PROTECTION CIRCUIT OF WIND POWER GENERATION SYSTEM

The super-capacitor model is usually simplified as ideal capacitor in series with the equivalent resistance model (Li and Xu, 2009; Dong *et al*., 2012). Crowbar super-capacitor circuit is constituted by the dc/dc bidirectional converter and an energy storage unit. When it is put into operation, the dc/dc bidirectional converter control the storage unit to charge/discharge and response fast to the over-voltage in dc side capacitor in grid voltage fault. Cut out crowbar super-capacitor circuit after grid voltage fault eliminates and wind power generation system quickly resume normal operation.

Figure 3 is Crowbar super-capacitor circuit topology, wherein R is load equivalent resistance, C_{dc} is dc capacitance values, U_{dc} is the bus voltage of dc capacitor, switches S_1 and S_2 are complementary breakover, L_1 is the inductor in the energy storage, i_{L1} is the inductor current, R_s is the equivalent resistance of

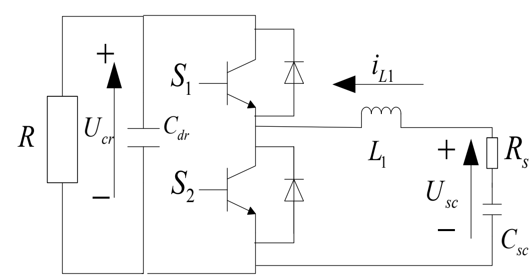

Fig. 3: The circuit topology of Crowbar super capacitor

the super-capacitor module, C_{sc} is the capacitance value of super-capacitor bank. In Fig. 3, the part from the super-capacitor to the dc side is boost circuit and the part from the dc side to the super-capacitor is buck circuit. When U_{dc} is lower than its rated value, the super-capacitor releases the extra energy and the circuit operates in boost condition; When U_{dc} is higher than its rated value, the super-capacitor absorbs the extra energy and the circuit operates in buck condition. Crowbar super-capacitors circuit controller detects the input and output active power value. The power difference is the primary judgment condition and the capacitor voltage in dc side is the auxiliary judgment condition when the crowbar super-capacitor circuit operates. Immediately enable crowbar super-capacitor when the power difference is reached the upper limit and calculate the duty cycle of the power switches according to control circuit. Fully and fast enable crowbar super-capacitor when the dc voltage reaches the upper limit. The crowbar super-capacitor is cut out

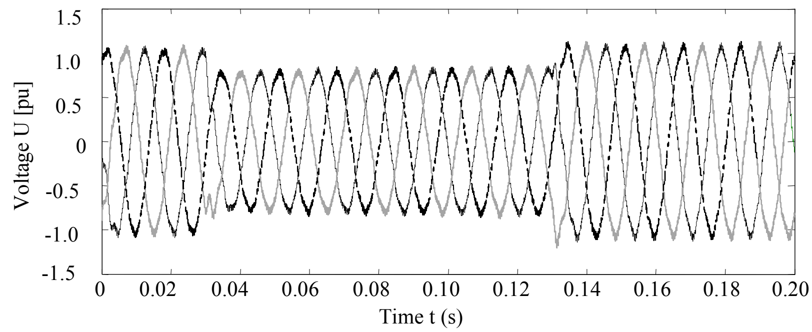

Fig. 4: Three phase voltages of the grid

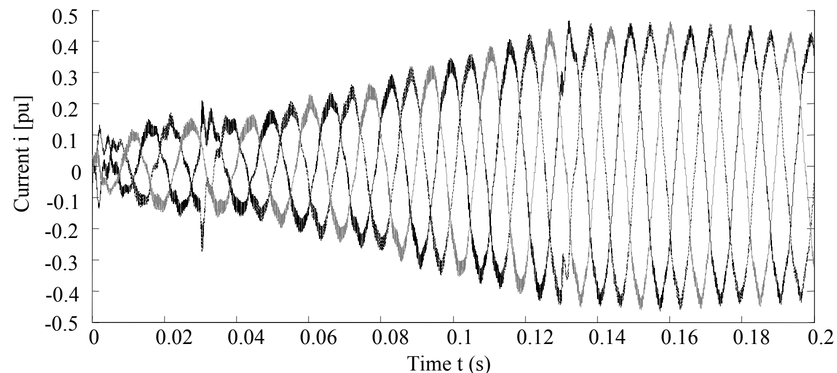

Fig. 5: Three phase currents of the grid

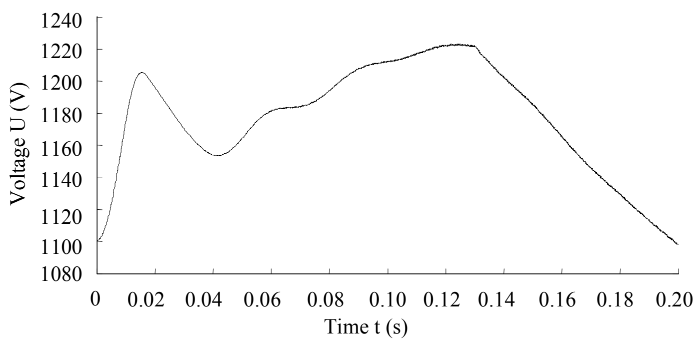

Fig. 6: The dc side voltage

when the power difference and the capacitor voltage meet the requirements. When dc side capacitor voltage as a condition controls crowbar super-capacitors to study, it is still the condition to control crowbar super-capacitor to cut out, otherwise two kinds of judgment conditions raise staggered impact. In order to avoid the crowbar super-capacitor frequently switching, control circuit should have hysteresis width.

SIMULATION RESULTS AND ANALYSIS

The wind power generation system consists of a synchronous generator connected to a diode rectifier, a DC-DC IGBT-based PWM boost converter and a DC/AC IGBT-based PWM converter. The power capacity is 10MW, the rated value of U_{dc} is 1100V and the referenced value of reactive power is 0 Mvar. (Fig. 4, 5 and 6)

The voltages and currents are per-unit values. At t = 0.03 s the positive-sequence voltage suddenly drops to 0.75 p.u. causing an increase on the dc capacitor voltage and a drop on the wind turbine output power. During the voltage sag the control systems try to regulate the dc capacitor voltage and reactive power at their set points (1100 V, 0 Mvar). The system recovers after fault elimination.

CONCLUSION

The asymmetric voltage and current can be decomposed into positive sequence, negative sequence and zero sequence components respectively via symmetrical component method. The methods proposed in this study can improve the asymmetric fault ride-through capability of wind power generation system, The mathematical models of grid side converter in static coordinate system and synchronous rotating coordinate system were given; predictive current control strategy proposed can achieve no static error tracking of current in each switching cycle, can eliminate the negative sequence current in asymmetric fault and wipe off the secondary ripple of the dc side capacitor voltage. The dc side super-capacitor circuit can prevent the dc side from over-voltage. The methods introduced in this study can improve the large grid asymmetric fault ride through capability of wind power generation system. From the simulation results given, effectiveness of the proposed methods is verified.

ACKNOWLEDGMENT

This study was supported in part by a grant from Project Supported by National Natural Science Foundation of China (51207002). Project Supported by Baoji University of Arts and Sciences (ZK11172, ZK11028) and Project Supported by Baoji City Science and Technology Bureau (11KG06-4).

REFERENCES

Chinchilla, M., S. Arnaltes and J.C. Burgos, 2006. Control of permanent-magnet generators applied to variable-speed wind-energy systems connected to the grid. IEEE T. Energy Convers., 21(1): 130-135.

Dong, L., X. Zhang, X. Huang, X. Liao *et al*., 2012. Analysis on power quality of grid-connected direct-driven wind power system with super capacitor storage energy. Trans. Beijing Inst. Technol., 32(7): 709-714.

Iov, F., A.D. Hansen, P. Sørensen and N.A. Cutululis, 2007. Mapping of gridfaults and grid codes. Risø National Laboratory, Technical University of Denmark, Roskilde, Denmark, Technical Report, Risø-R-1617(EN).

Jeon, J.H., S.K. Kim, C.H. Cho, J.B. Ahn and E.S. Kim, 2006. Developmentof simulator system for micro-grids with renewable energy sources. J. Elec. Eng. Technol., 1(4): 409-413.

Li, J. and H. Xu, 2009. Wind Power Generation System Low Voltage Ride through Technology. Mechanical Industry Press, China.

Lima, F.K.A., A. Luna, P. Rodriguez, E.H. Watanabe and F. Blaabjerg, 2010. Rotor voltage dynamics in the doubly fed induction generator during grid faults. IEEE T. Power Electron., 25(1): 118-130.

Polinder, H., F.F. Avan der Pijl and P. Tavner, 2006. Comparison of direct-driveand geared generator concepts for wind turbines. IEEE T. Energy Convers., 21(3): 543-550.

Saniter, C. and J. Janning, 2008. Test bench for grid code simulations for multi-MW wind turbines: Design and control. IEEE T. Power Electr., 23(4): 1707-1715.